An Integrated Geophysical Method Approach to Evaluating Managed Aquifer Recharge Potential in the Pilbara

Nathan Tabain
BHP
Nathan.tabain@bhp.com

Nicholas Quaglia
BHP
nicholas.quaglia@bhp.com

SUMMARY

A small detrital basin located in the Pilbara; WA was identified as a potential site for Managed Aquifer Recharge (MAR) of surplus water generated from nearby BHP mining operations.

To initially assess the potential of a site for MAR, a hydrogeological conceptual model is required, along with a subsequent exploration program to test key targets. Traditionally these objectives are primarily met by exploratory hydrogeological drilling to identify the depth to target injection stratigraphy, the location of major structure and dykes, and the thickness and potential clay-rich inclusions of detrital cover.

There was limited historical drilling available at the target location. However, several existing geophysical datasets were identified as covering most or all the target detrital basin. These consisted of an open-file airborne TDEM dataset and various mostly open-file airborne magnetic datasets. BHP also had a 2D seismic test line dataset.

The XTEM data was inverted, and a conductivity volume generated. This dataset identified the basal clays, a clay-rich layer typically found at the base of iron-rich detrital cover. A surface to the top of this anomaly was generated to assist with hydrogeological conceptualisation/modelling of different MAR scenarios.

The magnetic datasets were re-gridded, merged, filtered, and imaged. Key structures and dykes were then mapped from both the magnetic imagery and AEM derived depth-slices and iso-surfaces.

The 2D seismic section revealed a syncline-like feature in the cover-metasediment contact, the location of which coincided with an important structure identified from the EM and magnetic datasets, implying that the contact has been preferentially eroded along the structure.

These results ultimately translated to a reduction in required exploratory hydrogeological drilling to the effect of ~$500k, ~430 person-hours high-risk hazard exposure, reduced land clearing, and brought forward the timing of the knowledge acquired as the existing datasets did not require lengthy land access approvals.

Key words: Geophysics, Hydrogeology, AEM, Magnetic, Seismic

INTRODUCTION

The Pineapple Hill area is located in the Hamersley Basin in northern Western Australia. There is a small and shallow detrital basin located within the Pineapple Hill project area (Figure 1).

BHP West Australian Iron Ore (BHP WAIO) below water table mining operations require the abstraction of 10's of ML of groundwater per day per project (BHP, 2018). BHP WAIO has committed to returning much of its surplus ground water to the ground via managed aquifer recharge (MAR) (BHP, 2023). The Pineapple Hill detrital basin has been identified by BHP WAIO as a potential MAR target to support planned proximal future mining operations.

A hydrogeological conceptual model supported by test pumping data is required to study MAR options and maximise injection bore yields. The location and depth of target lithology including cover, as well as the presence of major structure and dykes are of particular interest. Traditionally information pertaining to these features of interest are primarily obtained via several phases of exploratory hydrogeological drilling. Exploratory hydrogeological drilling in remote areas is costly, hazardous and requires lengthy approvals processes and some land clearing.

Several existing geophysical datasets were identified in GSWA's MAGIX as covering most or all the target detrital basin. These consisted of an open-file airborne TDEM dataset (XTEM) and various mostly open-file airborne magnetic datasets. A confidential BHP WAIO airborne magnetic survey and 2D seismic line were also incorporated. There is limited shallow historical drilling available at the target location, along with LiDAR data and DMIRS geological map sheets.

Integration of these different datasets for hydrogeological interpretation was undertaken to determine if the existing and mostly open-file data could reduce the amount of planned costly and hazardous hydrogeological exploratory drilling, whilst reducing required land clearing and bringing forward the timing of the knowledge.

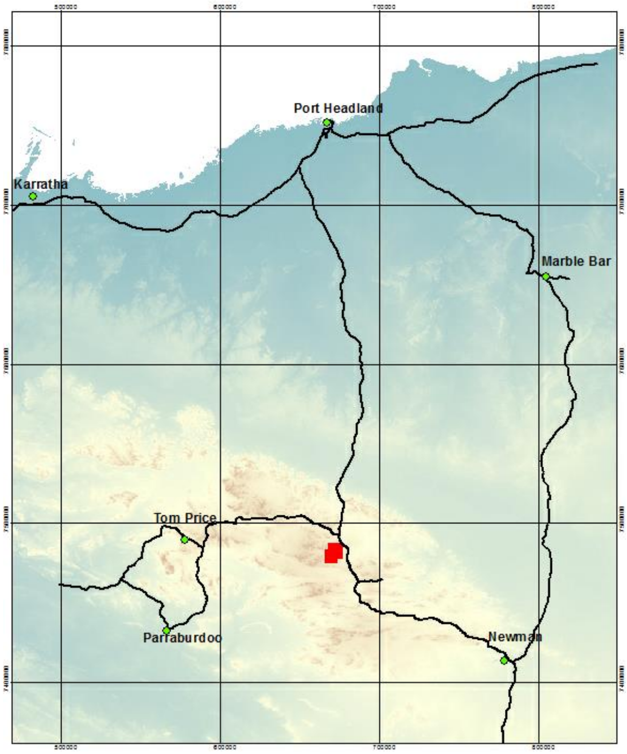

Figure 1. Map showing location of the Pineapple Hill project area. Red polygon represents AEM flight lines covering most of the area. Black lines show major roads. Green circles show major towns. False-colour image represents the digital elevation model.

GEOLOGICAL SETTING & SUPPORTING DATA

The geology of interest at Pineapple Hill consists of the meta-sediment Brockman Banded Iron Formation (BIF) to the west and Weeli Wolli BIF to the east, with the basin itself under detrital alluvium and colluvium cover consisting of silts, sands and gravels primarily composed of BIF, quartz and clays (DMIRS). When unoxidised, the BIFs are rich in magnetite (Trendall and Blockley, 1970). The base of the detrital cover sequence in the Hamersley Basin often consists of a clay-rich layer referred to as the "basal clay". Detrital cover has relatively high permeability, whilst BIF is highly dependent upon the presence of structure and/or mineralisation. The ground water within the Hamersley Basin is typically non-saline (BHP, 2023).

There is significant faulting and folding of the meta-sediments in the Hamersley Basin, with BHP WAIO recognising 5 different major events (Kerpert, 2001). Major structures are frequently intruded by dolerite dykes. Faults and joints can form either fluid pathways or barriers between different aquifers, with pathways being the more commonly encountered. Fresh dykes typically present as fluid barriers, creating aquifer compartments. Faults and joints are typically associated with weathering resulting in Magnetite oxidising to Hematite (Duuring et. al., 2019).

There is limited shallow historic drilling throughout the area targeting mineralisation of channel iron deposits located at the base of the detrital sequence, with the most recent drilling occurring in 1980. All drill holes were visually logged for lithology, and some have elemental assay data for a small portion of the hole targeting mineralised pisolites. There is no wireline geophysical data. Where drill data exists, detrital and pisolite cover thickness is interpreted to be a relatively consistent thickness varying from 50-60m, with basal clay interpreted beneath that with thickness up to 20m. Beneath cover was a mix of Brockman and Weeli Wolli BIF (west and east respectively) along with Dolerite. Several occurrences of potential faulting were noted. Drill holes were terminated as soon as they hit the underlying stratigraphy or intrusions.

GSWA 250k Geology map sheets were included in the analysis to help identify major lithologies throughout the basin setting.

A digital elevation model was generated from BHP WAIO LiDAR data at 5m resolution. This data is particularly valuable for locating structure and weathered dykes.

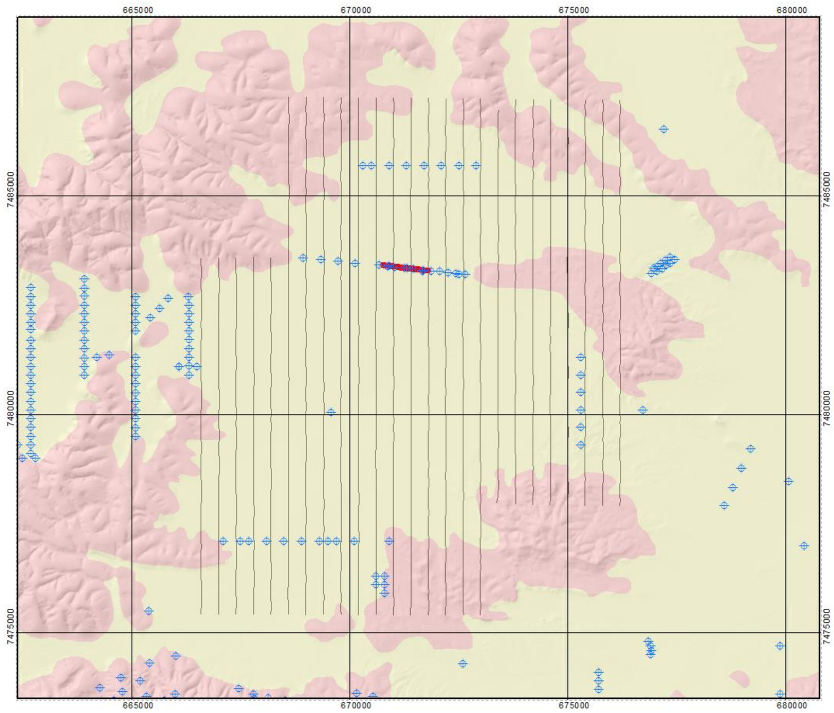

Figure 2. Map showing an overview of the different datasets. BIFs in pink and colluvium and alluvium in yellow (adapted from GSWA 250k map sheet), historical drilling in blue, 2D seismic line in red and AEM flight lines in black. Magnetic data covers the entire area. Base map consists of digital elevation model sun-shading.

ELECTROMAGNETIC DATA

Data from an open-file airborne electromagnetic XTEM survey was downloaded from DMIRS MAGIX. The survey was flown in 2010 and comprised of 284 km of data, with transverse lines flown at 400 m spacing and 000/180 degrees orientation. Nominal transmitter height was 35 m with 103,000 NIA.

The data were modelled in Geosoft VOXI TDEM 1D with the last four channels deselected and conductivity constraints applied. A mesh size of 100 m in the east-west direction was selected to take advantage of VOXI's interpolation-per-iteration capabilities to produce a final product that is easier to interpret across line, which was desirable given the relatively large flight-line spacing. The resulting conductivity volume was then clipped in the X and Y dimensions to remove mountainous areas surrounding the target detrital basin and clipped in the Z direction to remove all blocks <30 m from the surface to remove the shallow conductive anomaly frequently seen and believed to be caused by clay-rich alluvials. A Depth Of Investigation (DOI) surface was also derived from the contractor supplied pseudo-1D Conductivity Depth Image (CDI) data, and used to clip all blocks below this surface. The resulting conductivity model typically consists of a conductive layer sandwiched between resistors. The depth of investigation is interpreted as typically 100-150 m.

An iso-surface of the conductive layer was taken at 67 mS/m, and the top of this was converted to a grid showing the Relative Level (RL) to the top of the conductive anomaly. This grid was then subtracted LiDAR elevation data to generate a grid of depth to the top of the conductive anomaly. The average depth to the top of the conductive anomaly was approximately 55 m.

The conductivity block model was also sliced horizontally at various depths to assist with structural interpretation, with several major WSW-ENE features and a N-S feature being particularly evident.

Apparent depths to the top of the conductive anomaly increase significantly directly adjacent to outcropping BIF. This is likely due to the absence of the basal clays, resulting in the 67 mS/m iso-surface dropping down to the base of oxidisation where shales within and adjacent to the BIF stratigraphic layers become very conductive due to likely inclusion of disseminated sulphides (Zhan, 2022).

The data were also inverted in Mira VPem1D, which returned similar anomalies and conductivities. For this reason, the results were not interpreted separately and are not discussed further.

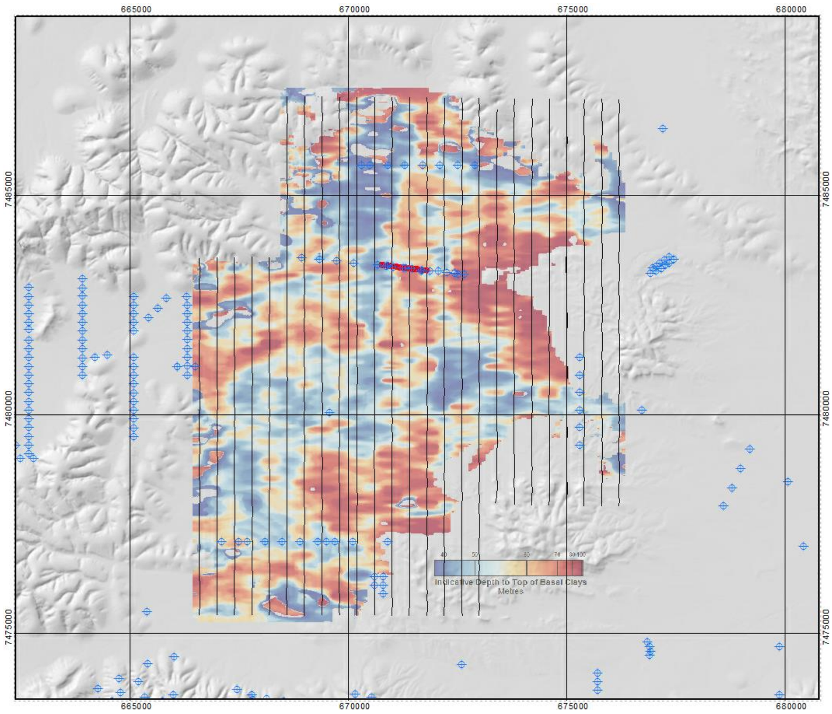

Figure 3. False-colour image depicts AEM derived indicative depth to the top of the basal clay. Depths typically range between 30 and 90 m. Historical drilling shown in blue, 2D seismic line in red and AEM flight lines in black. Base map consists of digital elevation model sun-shading.

MAGNETIC DATA

Data from three open-file airborne magnetic surveys were downloaded from GSWA's MAGIX. The surveys were flown from 1993 to 1997, at a line spacing of 200 to 300 m, at a nominal height of 80-100 m and all with a 000/180 degrees orientation. Data from a confidential BHP WAIO survey to the south was also included, which was flown in 2008 at 100 m line-spacing, 40 m nominal height and 000/180 degrees orientation.

The magnetic datasets were re-gridded, merged, filtered, and imaged. Of note was the inclusion of the Analytic Signal to account for remanent magnetism present in magnetite-rich BIF and maghemite-rich detritals, with remanence often resulting in strong magnetic intensity lows directly adjacent to strong highs in the Total Magnetic Intensity (TMI) and Reduction To Pole (RTP) data (Figure 4).

Key structures and intrusions were then identified from the magnetic imagery, with faults apparent from offset in the magnetic stratigraphy, joints evident from demagnetisation of magnetic stratigraphy, and potential dykes evident as remanently magnetic linear anomalies.

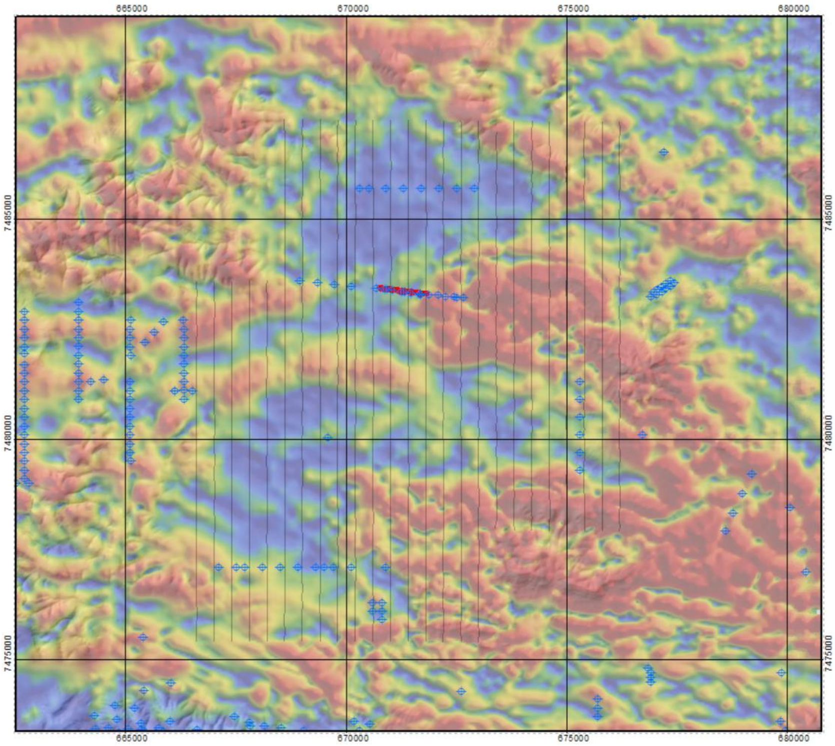

Figure 4. False-colour image depicts the Analytic Signal of the TMI. Historical drilling shown in blue, 2D seismic line in red and AEM flight lines in black. Base map consists of digital elevation model sun-shading.

SEISMIC DATA

A ~1km long 2D seismic survey was conducted by Curtin University on behalf of BHP WAIO along a track hosting historic drillholes. Receivers consisted of 3-component geophones at 5m spacing and various Distributed Acoustic Sensing (DAS). Source points were also 5m apart along most of the line and consisted primarily of a 40kg accelerated weight drop firing five time per shot location. The results from the DAS will not be discussed here.

The processed seismic data revealed a single dominant contact underneath a highly attenuative zone interpreted to be the contact between the cover and the underlying meta-sediment BIF's. The contact presents as a broad, smooth channel-like feature in the DMO stack, and a more structurally complex result in the CMP stack. Constant Velocity Stacks (CVS) analysis was used to derive a velocity of 2,500 m/s. However, this simplistic approach risks over-estimating the velocity of the overlying cover by focusing on the features associated with the underlying stratigraphy. In both the DMO and CMP data, the depth at the keel of the channel-like feature is approximately 250m and several hundred metres wide, whilst the depth to the top of the adjacent relatively flat contact is around 120m.

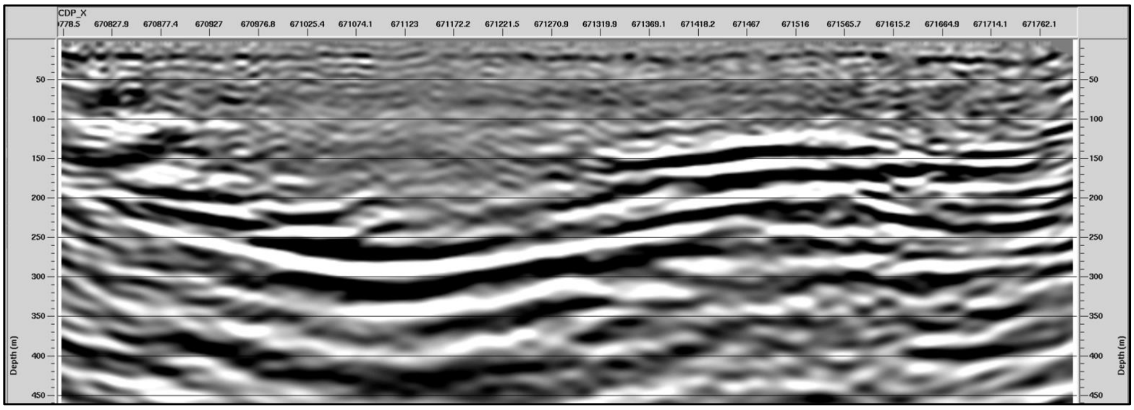

Figure 5. Image of the depth migrated DMO stack seismic data. A channel-like feature is visible down to an apparent depth of 250m.

INTEGRATED INTERPRETATION OF GEOPHYSICAL DATA

Interpreting any one of the geophysical datasets in isolation does provide value, however the problem of equivalence, and of the potential for geological features having insufficient physical property contrasts results in relatively high uncertainty in any interpretations made. There is also the potential for oversimplification of data processing workflows to impact the accuracy of subsequent interpretations.

Instead, the different geophysical method datasets, accompanied by other relevant datasets such as LiDAR and surface mapping can be incorporated together into a joint interpretation, all of which is controlled by limited drill data. This reduces the significance of equivalence by allowing multiple physical properties and/or contrasts to be measured for a given stratigraphy or structure. Subtle features which are repeated by two or more datasets reduces uncertainty. Ultimately this approach allows for a greater number of hydrogeological features to be identified, whilst simultaneously increasing confidence in the data. Such an approach is discussed in Isles, 2013.

The depth to the top of the basal clay was estimated from the inverted AEM data and can be validated against the 2D seismic section, both of which can then be validated against the limited shallow drill data. The unconstrained AEM inversion results show an average depth to top of conductive anomaly of 55 m, aligning with the drill lithology logging which shows the top of the basal clay as typically being 50-60 m deep (Figure 6). This correlation with drilling provides confidence in the extrapolation of the interpretation of the top of the basal clay from the inverted AEM data throughout the basin. The interpreted top of the basal clay surface informs the hydrogeological conceptual model of the indicative overlying detrital cover thickness and depth to the top of the underlying BIF throughout most of the target basin, both of which are key to determining MAR storage potential. This surface is also a valuable tool in informing optimal planned drill depths.

The seismic dataset typically shows depth to basement BIF and dolerite from 120-250 m depth, which is significantly deeper than indicated by the drilling along the same line of 50-80 m (Figure 6). This is likely due to the utilisation of a CVS velocity derived from the basement stratigraphy being applied to the overlying cover. If a velocity of 1,000 m/s were used for cover, this would return depths of 50-100 m which would align well with the AEM and drill data. This lower value also better aligns with velocities derived from cover at other trial seismic surveys BHP WAIO has recently acquired. Whilst the AEM cannot image this contact accurately as it resides at the base of a conductor, a synclinal shape is evident that largely mirrors that of the seismic reflection image, were it compressed by a factor of 2.5 times to incorporate the lower cover velocity. The easting of the syncline like feature visible in the 2D seismic and unconstrained AEM inversion results correlate well with a subtle large-scale N-S lineament visible in the airborne magnetic data. The various datasets all suggesting the presence of thicker cover at this location, potentially the result of a weathered fault or dyke. This features also aligns with modern day drainage of the basin to the north between topographic highs and is a key target for hydrogeological drilling given it presents as an attractive injection target.

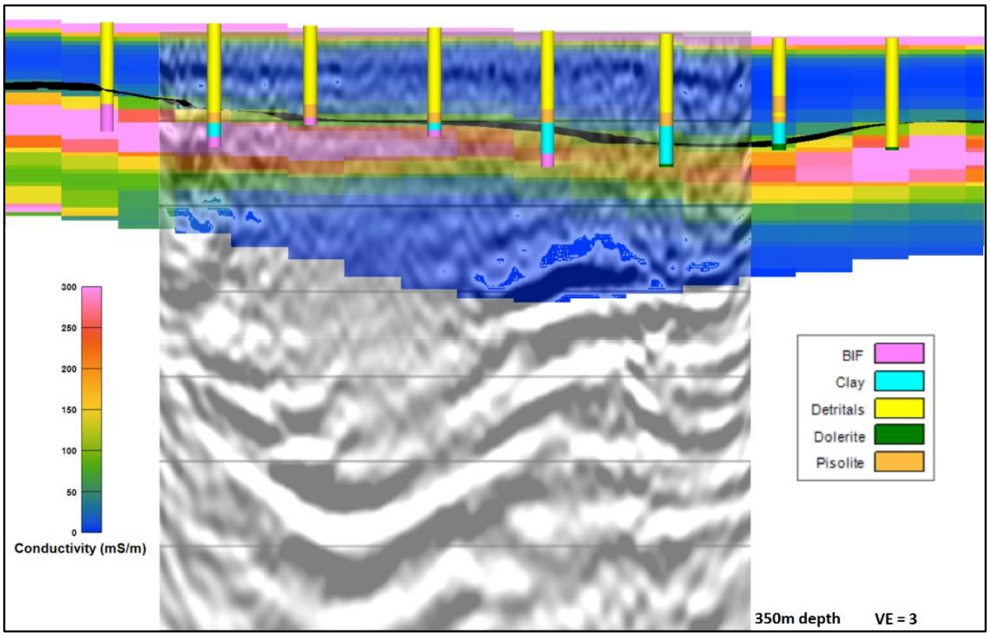

Figure 6. Interpreted depth to top of “basal clay” derived from AEM data shown in black. Crossline section of the conductivity model represented as false-colour image. Seismic reflection depth-section shown as grey-scale. Drill hole lithology shown as coloured cylinders. Note the correlation between the interpreted depth to top of basal clay with the drill derived lithology. Also note the stratigraphy imaged by the seismic is much deeper than that intercepted by drilling, suggesting cover has lower velocities.

Potential large faults, joints and dykes identified in the airborne magnetics can be validated against all the other incorporated datasets discussed: the inverted AEM data showing lineaments with increased depth to the top of the basal clay, the weathered paleo-channel like feature visible in the seismic, surface mapping and limited drill data. Figure 7 depicts an interpreted N-S structure, evident in the magnetic data, which intersects the “syncline-like” feature in the seismic line, aligns with the boundary between deep cover to the east and shallow cover to the west derived from the AEM data, and agrees with the location of a potential fault identified in drill data. Elsewhere magnetic lineaments align with discrete erosional lineaments visible in the Digital Elevation Model, suggesting the presence of structure that have resulted in oxidisation of magnetite to hematite.

These structures represent excellent hydrogeological exploration drill targets to test both the targets presence and significance to the basin’s storage potential, given their potential to represent not only fluid conduits above basement via the presence of thicker detrital cover, but for the potential for these structures to represent zones of increased permeability within the stratigraphic basement below, further improving MAR potential.

Figure 7 also depicts 2 large, interpreted WSW-ENE dykes and 2 smaller N-S dykes visible in the middle of the airborne magnetic data as linear features with very low amplitudes in the RTP TMI grids and high amplitudes in the Analytical Signal grid suggesting strong remanent magnetism. Several drillholes along the seismic test line were interpreted to intercept dolerite basement. These anomalies also align with linear zones of greater cover thickness interpreted in the AEM data suggesting basement erosion.

As with the interpreted structures, the interpreted dykes represent ideal exploration drill targets to test for potential compartmentalisation of the underlying stratigraphic aquifers. If confirmed, these features can have significant impacts on the calculated MAR potential in terms of annual injection rates, localised mounding and to identify any potential down-gradient areas which may require additional knowledge gathering.

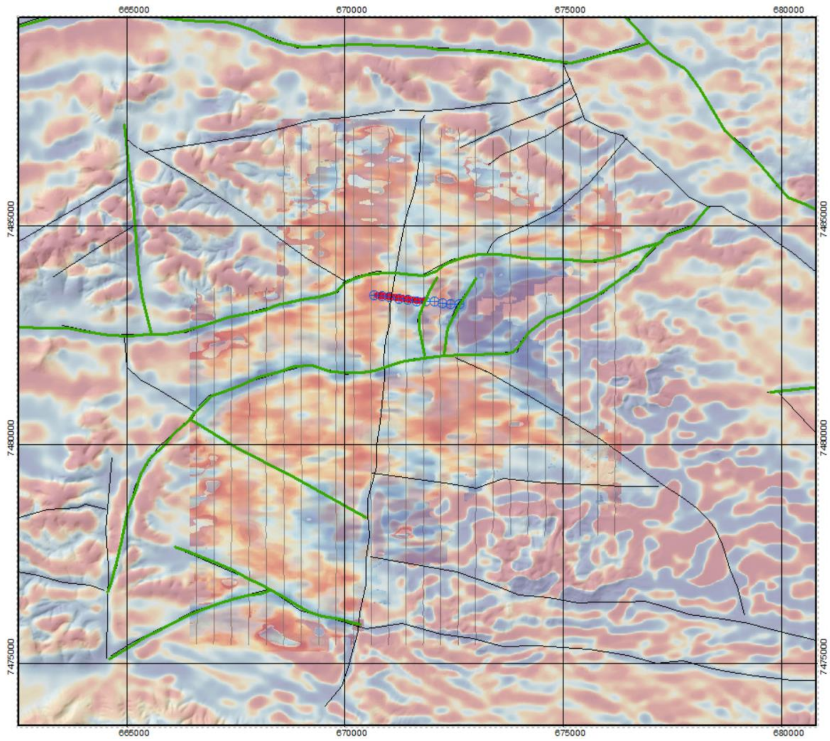

Figure 7. Interpreted major structure shown as black lines and dykes as green lines. Inverse heat map of depth to top of basal clay derived from AEM data (hot = shallow) shown on top of heat map of the 1VD of the RTP TMI shown on top of a sun-shading grid of the digital elevation model. AEM flight lines shown in grey, seismic line in red and drill holes shown in Figure 6 as blue circles. Note that thicker cover correlates well with low amplitude 1VD_RTP_TMI data.

Upon review of the products generated from the joint-interpretation of the discussed datasets, and subsequent creation of a conceptual hydrogeological model, the magnitude of the exploration hydrogeological drilling typically required for a MAR target such as Pineapple Hill was scaled back. Not only was some of the required information obtained without the need for drilling on-tenure, but information was also obtained off-tenure. Furthermore, most of this data was freely available and ready to model and interpret.

CONCLUSIONS

Geophysical data, including open-file data, can be integrated along with other non-geophysical datasets to identify target geology, structure and dykes which are crucial to the hydrogeological conceptualisation of potential MAR basins. The integration of the different datasets can help reduce non-uniqueness associated with any singular dataset and improve confidence in the interpretations generated.

The hydrogeological information interpreted from the mostly open-file geophysical data reduced the required number of exploratory hydrogeological drilling to the effect of ~$500k drilling and earthworks costs, ~430 person-hours high-risk drilling and remote travel hazard exposure, and reduced land clearing from less drill pads and access pads. The geophysical derived interpretation also brought forward the timing of the hydrogeological conceptualisation and subsequent drill planning as utilisation of the existing datasets did not require lengthy land access approvals. The data acquired off-tenure is invaluable.

This integrated geophysical method approach to generating hydrogeological conceptual data for MAR has been utilised by BHP WAIO at numerous other locations across the Pilbara utilising in-house high-resolution AEM, airborne magnetic and airborne gravity gradiometry datasets with reasonable success. This case-study highlights how the same approach can be somewhat successful utilising mostly open-file data and should be replicated where possible for MAR conceptualisation.

ACKNOWLEDGMENTS

I would like to thank Nicholas Quaglia for his contributions to this extended abstract, Curtin University for acquiring and processing the seismic data, GSWA for enabling easy identification and downloading of open-file geophysical datasets in Western Australia, and finally BHP WAIO for allowing me to publish this work.

REFERENCES

BHP, 2018, Managing excess water in the Pilbara: https://www.bhp.com/news/case-studies/2018/08/managing-excess-water-in-the-pilbara.

BHP, 2023, Water: https://www.bhp.com/sustainability/environment/water.

DMIRS - State of Western Australia (Department of Mines, Industry Regulation and Safety) 2022: 1:250k geological map – Roy Hill (SF50-12), second edition.

Duuring P., Steffen G., Hagemann, Laukamp C, Chiarelli L., 2019, Supergene modification of magnetite and hematite shear zones in banded iron-formation at Mt Richardson, Yilgarn Craton, Western Australia, Ore Geology Reviews, Volume 111.

Isles, D.J, and Rankin, L.R, 2013, Geological Interpretation of Aeromagnetic Data: Australian Society of Exploration Geophysicists.

Kepert, D.A., 2001. The mapped stratigraphy and structure of the Mining Area C region: Geological Survey of Western Australia, Report 185.

Zhan, Y. 2022. Airborne Electromagnetic Survey, Northern Western Australia: An Integrated Interpretation Of Selected Features, Report 234.